crystals

MDPI

Article

Displacements in the Cationic Motif of Nonstoichiometric Fluorite Phases $Ba_{1-x}R_xF_{2+x}$ as a Result of the Formation of $\{Ba_8[R_6F_{68–69}]\}$ Clusters: III. Defect Cluster Structure of the Nonstoichiometric Phase $Ba_{0.69}La_{0.31}F_{2.31}$ and Its Dependence on Heat Treatment †

Elena A. Sulyanova *, Denis N. Karimov and Boris P. Sobolev

Shubnikov Institute of Crystallography, Federal Scientific Research Centre “Crystallography and Photonics”, Russian Academy of Sciences, Leninskiy Prospekt 59, 119333 Moscow, Russia; dnkarimov@gmail.com (D.N.K.); sobolevb@yandex.ru (B.P.S.)

* Correspondence: sulyanova@gmail.com

† In memory of A.M. Golubev.

Abstract: The defect structure of $Ba_{0.69}La_{0.31}F_{2.31}$ single crystals in as-grown state and after annealing at 1173 K for 336 h was studied by X-ray diffraction analysis. Both crystals belong to the CaF_2 structure type (sp. gr. $Fm\bar{3}m$). They have vacancies in the main anion motif and interstitial fluorine anions in Wyckoff positions 48*i* and 4*b*. Relaxation (static displacement of some main anions to Wyckoff position 32*f*) is observed in the annealed crystal. It was established that annealing leads to a change in the type of displacement of the main anions in Wyckoff positions 8*c* from dynamic to static. Displacement of La^{3+} cations to Wyckoff position 32*f* is observed in both crystals. A model of the defect structure of $Ba_{0.69}La_{0.31}F_{2.31}$ is proposed, according to which interstitial fluorine anions and La^{3+} cations are aggregated into $[Ba_{14-n}La_nF_{64+n}]$ clusters with the cuboctahedral anionic core formed by interstitial fluorine anions in Wyckoff positions 48*i*. Ba^{2+} cations are located in the cluster in the centers of the faces, and the La^{3+} cations are shifted by 0.24 Å from the vertices of the cluster along the three-fold axis towards the center of the cluster. The study establishes the relationship between the defect structure of crystals and their structurally sensitive properties, and to develop approaches to their management.

Keywords: nonstoichiometric fluorides; defect crystal structure; clusters; rare earths; fluorite

check for updates

Citation: Sulyanova, E.A.; Karimov, D.N.; Sobolev, B.P. Displacements in the Cationic Motif of Nonstoichiometric Fluorite Phases $Ba_{1-x}R_xF_{2+x}$ as a Result of the Formation of $\{Ba_8[R_6F_{68–69}]\}$ Clusters: III. Defect Cluster Structure of the Nonstoichiometric Phase $Ba_{0.69}La_{0.31}F_{2.31}$ and Its Dependence on Heat Treatment. *Crystals* **2021**, *11*, 447. https://doi.org/10.3390/cryst11040447

Academic Editor: Nataliya Novikova

Received: 14 March 2021
Accepted: 17 April 2021
Published: 20 April 2021

1. Introduction

One of the ways of searching for new crystalline materials is the complication of a chemical composition of crystals with saving of their structure type. Namely, with the transition to an isostructural solid solution, some physical characteristics vary within a wide range. This approach allows one to efficiently control the physicochemical properties and expands the range of promising crystalline materials for various areas of solid-state physics and chemistry. The nonstoichiometric phases $M_{1-x}R_xF_{2+x}$ (M = Ca, Sr, Ba; R = rare earth elements) with the defect fluorite structure are the most commonly used and promising materials in technological applications among known fluoride nonstoichiometric phases. They are formed in 80 MF_2–RF_3 systems [1]. The $M_{1-x}R_xF_{2+x}$ phases have different properties compared to the initial MF_2, due to their structural features.

According to the modern concept about the structure of nonstoichiometric fluorite phases $M_{1-x}R_xF_{2+x}$, the defects formed as a result of heterovalent isomorphic replacement of M^{2+} cations by R^{3+} cations are grouped into clusters. The anion core of the clusters consists of interstitial anions. According to the principle of local charge compensation, the impurity cations R^{3+} are located around the anion core to form cation–anion clusters [2–5].

The presence of vacancies in the main anionic motif and interstitial anions in one or more positions is considered to be evidence of cluster formation in the disordered $M_{1-x}R_xF_{2+x}$ phases. The cuboctahedral groups $\{F_{12}\}$ formed by fluorine anions in Wyckoff site 48*i* (sp. gr. $Fm\overline{3}m$) are cores of cation–anion octacubic clusters $[M_{14-n}R_nF_{64+n}]$ (Figure 1). The study of the cluster structure based on data on interstitial anions is associated with methodological difficulties in determining light fluorine anions against the background of heavy barium and rare earth cations. The accuracy of determining the occupancies of the positions occupied by the interstitial anions in the $M_{1-x}R_xF_{2+x}$ structure is quite low.

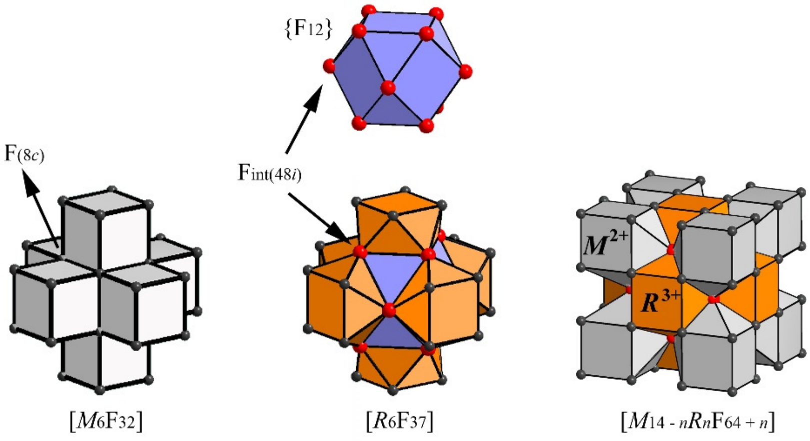

(**a**) (**b**) (**c**)

Figure 1. (**a**) The fragment $[M_6F_{32}]$ of the fluorite structure formed by M^{2+} cations and matrix fluorine anions $F_{(8c)}$ in Wyckoff positions 8*c* at ($\frac{1}{4}$, $\frac{1}{4}$, $\frac{1}{4}$). (**b**) Cuboctahedron $\{F_{12}\}$, formed by interstitial fluorine ions $F_{\text{int}(48i)}$ in Wyckoff positions 48*i* at (u, u, $\frac{1}{2}$), and the octahedral $[R_6F_{37}]$ cluster. (**c**) Octacubic cluster $[M_{14-n}R_nF_{64+n}]$ [4,5].

In early studies of the defect structure of the $M_{1-x}R_xF_{2+x}$ phases, Wyckoff position 4*a* was assumed to be fully occupied with the statistical mixture of the cations ($M_{1-x}R_x$) [6]. The reason for this was use of a limited data set, which allowed for localizing interstitial fluorine ions but did not enable to reveal tiny features of a structure such as anharmonic vibrations of ions and displacement of cations from the Wyckoff position 4*a*. For the first time, the splitting of the cationic crystallographic Wyckoff site 4*a* in the disordered fluorite phases $M_{1-x}R_xF_{2+x}$ was detected by us in $Ba_{0.75}Lu_{0.25}F_{2.25}$ [7].

The tendency toward the positional differentiation is enhanced with an increase in a difference between the ionic radii of the M^{2+} and R^{3+} cations. The $Ba_{1-x}R_xF_{2+x}$ (R = Tm − Lu) solid solutions are characterized by a maximum difference in the sizes of M^{2+} and R^{3+} cations. We found that in such phases the differentiation of the positions of cations is expressed in a formation of the ordered phases $Ba_4R_3F_{17}$ (R = Y, Yb) [8] with a fluorite-related structure that are formed in the BaF_2–RF_3 systems with R = Sm–Lu. In such phases the octacubic clusters transform from disordered defects into elementary structural units (Figure 2). Long-range order emerges in the spatial arrangement of the clusters.

The cationic motif of the ordered phases is trigonally distorted. Different types of cations occupy various positions, which make it possible to determine their displacements from ideal fluorite positions. The accuracy of determining the cluster structure of the nonstoichiometric phases $M_{1-x}R_xF_{2+x}$ based on anionic defects alone is low. The possibility of involving displacements of cations in the refinement of the cluster structure enables one to increase the reliability of the model of the defect structure. For many years, A.M. Golubev successfully developed the idea of extending the cluster structure of ordered phases with a structure derived from the fluorite to the structure of disordered fluorite phases $M_{1-x}R_xF_{2+x}$. The idea is based on the connection between the splitting of the cationic position and the formation of the octacubic clusters.

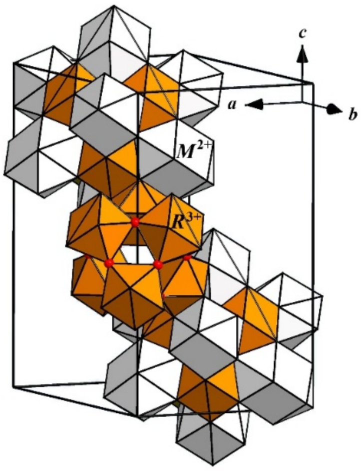

Figure 2. The octacubic $[M_{14-n}R_nF_{64+n}]$ clusters in the $M_4R_3F_{17}$ structure.

This work is a continuation of a series of studies [4,5] on the investigation of the displacements of cations in the disordered $Ba_{1-x}R_xF_{2+x}$ (R = La–Lu) phases. The goal of the study is to complete the investigation of the cationic displacements in $Ba_{1-x}R_xF_{2+x}$ crystals for the entire rare earth range from La to Lu. This is achieved by selecting the $Ba_{1-x}La_xF_{2+x}$ crystal containing the first member of the rare earth series—La—as the object of this work.

A specific feature of the fluorite phases $Ba_{1-x}R_xF_{2+x}$ is congruent melting. Such behaviour is anomalous and found only for heterovalent solid solutions with a variable number of atoms in the unit cell. The formation of maxima on $Ba_{1-x}R_xF_{2+x}$ melting curves was found by [9] using the differential thermal analysis method for the BaF_2–RF_3 systems with R = La–Tb. A rise in the melting point of the congruently melting phase $Ba_{0.69}La_{0.31}F_{2.31}$ (by 130 K with respect to the melting point of the BaF_2) is the maximum among all congruently melting $M_{1-x}R_xF_{2+x}$ phases.

The $Ba_{0.69}La_{0.31}F_{2.31}$ bulk crystals of optical quality can be grown from the melt due to a congruent melting. They are of practical importance as a potential wide band-gap optical material with improved characteristics (compared to the commercially produced BaF_2 single crystals) [10] and have increased mechanical strength and significant deterioration of cleavage. The possible application of these crystals in a heating–cycling mode requires an understanding of the behavior of their structure during heat treatment. Therefore, a structural study of the $Ba_{0.69}La_{0.31}F_{2.31}$ crystals annealed at 1173 K for a long time was also performed.

2. Materials and Methods

The $Ba_{0.69}La_{0.31}F_{2.31}$ single crystal was grown by the Bridgman technique from a melt. The anhydrous BaF_2 and LaF_3 (99.99%, LANHIT) powders were used as raw materials. The powders were preliminarily annealed in vacuum (~10^{-2} Pa) for 3–5 h at 450 K and then remelted in a fluorinating CF_4 atmosphere. The growth equipment with resistive a graphite heating system and multicellular graphite crucible was applied.

The temperature gradient in the growth zone was ~100 K/cm, crucible pulling rate—5 mm/h and cooling rate of grown crystals ~100 K/h. CF_4 (99.999%) was used as a fluorinating agent during growth. $Ba_{0.69}La_{0.31}F_{2.31}$ single crystals of optical quality were successfully grown with these growth process parameters. Loss of the substance during the crystallization process was about 1 wt.%; no cracks or light-scattering centers were observed.

Postgrowth annealing of $Ba_{0.69}La_{0.31}F_{2.31}$ crystals was performed in a growth facility at 1173 ± 20 K for 336 h. A fluorinating atmosphere was formed by CF_4. The sample for annealing was cut from the middle part of the as-grown crystalline boule ($\sim$0.5 cm^3), wrapped in a Ni foil and placed in a graphite crucible. It was located in the near-zero-gradient area of the heater (the axial temperature gradient was less than 5 K/cm). At the end of the heat treatment process, the crucible was cooled by turning off the heater supply and passing a continuous flow of inert gas at room temperature through the volume of the growth chamber. The cooling rate in the initial stage was estimated to be about 200 K/min.

The details of the X-ray diffraction experiment (Xcalibur S Agilent Technologies (Oxford Diffraction), Poland) are listed in Table 1. An analysis of the diffraction data showed that both crystals belong to the CaF_2 structure type.

Table 1. Details of the X-ray diffraction experiment, structure refinement and crystal data for $Ba_{0.69}La_{0.31}F_{2.31}$.

	As-Grown	**Annealed**
Crystal syst., sp.gr., Z	Cubic, $Fm\bar{3}m$, 4	
a (Å) [1]	6.1087 (5)	6.1150 (5)
V (Å^3)	227.95 (5)	228.66 (5)
D_x (g·cm^{-3})	5.2947 (5)	5.2784 (5)
Wavelength (Å)	0.71073	
T (K)	295	
μ (mm^{-1})	17.55	17.50
$T_{\min}$, $T_{\max}$	0.0954, 0.1946	0.1178, 0.2155
Crystal size, diameter (mm)	0.20	0.18
Shape, Color	Sphere, colorless	
Diffractometer	Xcalibur S Oxford Diffraction	
Θ range (deg)	5.78–73.62	
Coverage (%)	100	
Limiting indices	$-16 < h < 16$, $-15 < k < 15$, $-16 < l < 16$	
Refl. collected/unique, R_{int}	5589/157, 0.0424	5577/157, 0.0569
Refinement method [2]	Full matrix least squares on F^2	
Data/restraints/param	157/1/14	157/1/16
R/wR, %	0.82/2.12	0.96/2.25
Goodness of fit	1.00	1.00
$\Delta\rho_{\min}/\Delta\rho_{\max}$, e/Å^{-3}	−0.34/0.39	−0.37/0.38

[1] Unit-cell parameters were calculated based on X-ray powder diffraction patterns. [2] JANA2006 weighting scheme [11] applied to X-ray data, $\omega = 1/(4F^2[\sigma^2(|F|) + (0.008 \cdot F)^2])$.

The structure was refined within the sp. gr. $Fm\bar{3}m$ using the JANA2006 program [11]. During refinement, an isotropic extinction correction was introduced into the fitted model according to the Becker–Coppens formalism [12] (type I, angular distribution of mosaic blocks according to the Gaussian law). When refining the anharmonic components of atomic displacement tensor, the temperature factor was expanded in Gram–Charlier series [13].

3. Results

Using the method of structural analysis of the $M_{1-x}R_xF_{2+x}$ phases, it was found that interstitial fluorine anions appear in difference Fourier syntheses in eight Wyckoff positions: four 32*f* (w, w, w), two 48*i* (u, u, 0.5), 48*g* (q, 0.25, 0.25), 24*e* (p, 0.5, 0.5) and 4*b* (0.5, 0.5, 0.5) sp. gr. $Fm\bar{3}m$. The Wyckoff system is used to denote the anions in our work $F_{\text{int(position)}s}$; *s* is indicated for the difference of anions in the same position with different coordinates. The matrix anion in Wyckoff site 8*c* is denoted as $F_{(8c)}$.

The difference Fourier electron density maps for as-grown and annealed $Ba_{0.69}La_{0.31}F_{2.31}$ single crystals in the (110) plane are shown in Figure 3. The solid, dotted and long dashed lines in the maps indicate, respectively, positive, negative and zero electron densities. The coordinate grid is given in unit cell fractions. Differences were obtained by subtracting the contributions of ions, Ba^{2+} and La^{3+} cations, which share the 4*a* site in the structure, and matrix anions $F_{(8c)}$ occupying the Wyckoff position 8*c* with refined site occupancy. All atomic displacement parameters were refined in the harmonic approximation.

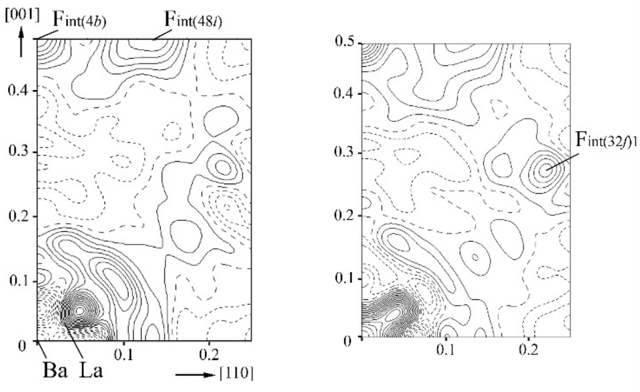

(**a**) (**b**)

Figure 3. Difference electron-density maps of as-grown (**a**) and annealed (**b**) $Ba_{0.69}La_{0.31}F_{2.31}$ crystals in the (110) plane. Isolines are given with a step of 0.1 e/Å^3.

The difference maps shown in Figure 3 exhibit pronounced electron density maxima corresponding to interstitial fluorine ions. The maxima in Wyckoff sites 48*i* and 4*b* are present in the maps of both crystals, which belong to interstitial fluorite ions $F_{int(48i)}$ и$F_{int(4b)}$, respectively. The maximum in 32*f* in the map of the annealed crystal corresponds to statically displaced matrix $F_{(8c)}$ anions, which were denoted as $F_{int(32f)1}$. The process of shifting matrix anions from their positions is called anionic sublattice relaxation.

The analysis of the displacement of atoms from their crystallographic positions consists in the evaluation of the harmonic and anharmonic thermal vibrations (dynamic displacements) and the analysis of the real displacements (static displacements), which are referred to as the splitting of crystallographic positions. The criterion for applicability of a particular approach is the discrepancy factor.

The character of electron density distribution near the site of the matrix anion $F_{(8c)}$ in the difference map of the as-grown $Ba_{0.69}La_{0.31}F_{2.31}$ crystal (Figure 3a) suggests dynamic displacements of matrix anions. The consideration of anharmonicity of thermal vibrations of $F_{(8c)}$ anions in this crystal to the third order of expansion in the structure refinement led to complete elimination of the electron density maximum and minimum near the site of the $F_{(8c)}$ anion in the as-grown phase. In the annealed crystal, the consideration of anharmonicity of thermal vibrations of $F_{(8c)}$ anion did not lead to any changes in the difference map; thus, it is likely that only static displacements of $F_{(8c)}$ anions exist in this case.

The distribution of the electron density near the cation position in both crystals (Figure 3) is characteristic of the static displacement of a part of the cations from Wyckoff position 4*a* to 32*f*. The attempt to refine the model with the part of Ba^{2+} cations being displaced in 32*f* was unsuccessful. Implementation of the anharmonic displacement model to thermal vibrations of Ba^{2+} and La^{3+} cations sharing the 4*a* position did not eliminate the maxima and minima of the electron density near the cation position either. The displacement of all La^{3+} cations to Wyckoff site 32*f* and application of the anharmonic approximation for the thermal oscillations of Ba^{2+} cations led to elimination of all heterogeneities in the electron density distribution near Wyckoff site 4*a* in the difference Fourier maps of both as-grown and annealed crystals.

In the last stage of refinement, the total number of anions was fixed in correspondence with the composition of each crystal. The coordinates, site occupancy factors and equivalent atomic displacement parameters in the crystals under study are given in Table 2.

Table 2. Wyckoff position (*W. p.*), site occupancy factors (*s. o. f.*), fractional coordinates and equivalent isotropic thermal displacement parameters of atoms in as-grown and annealed $Ba_{0.69}La_{0.31}F_{2.31}$ crystals.

Thermal State	Ion	*W. p.*	*s. o. f.*	*x/a*	*y/b*	*z/c*	B_{eq}
as-grown	$Ba_{(4a)}$	4*a*	0.690	0	0	0	0.985 (4)
	$La_{(32f)}$	32*f*	0.039	0.0229 (2)	0.0229 (2)	0.0229 (2)	0.60 (2)
	$F_{(8c)}$	8*c*	0.777	$\frac{1}{4}$	$\frac{1}{4}$	$\frac{1}{4}$	2.04 (1)
	$F_{int(48i)}$	48*i*	0.059 (7)	0.129 (3)	0.129 (3)	$\frac{1}{2}$	2.9 (3)
	$F_{int(4b)}$	4*b*	0.048 (8)	$\frac{1}{2}$	$\frac{1}{2}$	$\frac{1}{2}$	2.5 (9)
annealed	$Ba_{(4a)}$	4*a*	0.690	0	0	0	0.954 (5)
	$La_{(32f)}$	32*f*	0.039	0.0226 (3)	0.0226 (3)	0.0226 (3)	0.67 (3)
	$F_{(8c)}$	8*c*	0.771	$\frac{1}{4}$	$\frac{1}{4}$	$\frac{1}{4}$	2.16 (6)
	$F_{int(32f)1}$	32*f*	0.007 (2)	0.286(4)	0.286 (4)	0.286 (4)	0.66 (8)
	$F_{int(48i)}$	48*i*	0.057 (8)	0.124(5)	0.124 (5)	$\frac{1}{2}$	3.6 (9)
	$F_{int(4b)}$	4*b*	0.028 (8)	$\frac{1}{2}$	$\frac{1}{2}$	$\frac{1}{2}$	1.4 (8)

The atomic displacement parameters of the $F_{(8c)}$ anion in as-grown crystal and Ba^{2+} cation in both crystals were refined within the anharmonic approximation to the third and fourth order of expansion, respectively. The standard deviations for the site occupancies of each atom were calculated with the other refined parameters being fixed.

4. Discussion

According to [9], no ordered phases were detected in the BaF_2–LaF_3 system. Strictly speaking, one cannot apply any model of an ordered phase for building a model of a structure of the disordered phase $Ba_{0.69}La_{0.31}F_{2.31}$. Besides, disordered fluorite phases $M_{1-x}R_xF_{2+x}$, in contrast to ordered ones $M_mR_nF_{2m+3n}$, are in a nonequilibrium state. Therefore, the structural unit of the ordered phases may not be strictly repeated in the disordered ones.

Let us assume that the structural model of $Ba_{0.69}La_{0.31}F_{2.31}$ crystal is based on the octacubic cluster $[Ba_{14-n}La_nF_{64+n}]$, which is an elementary structural unit in $Ba_4R_3F_{17}$ phases. On the basis of a structure of the ordered phase $Ba_4R_3F_{17}$, it is possible to propose the formation of anionic groups $\{F_{12}\}$ in nonstoichiometric disordered phase $Ba_{0.69}La_{0.31}F_{2.31}$, which are formed by $F_{int(48i)}$ anions. The ratio of the number of vacancies ($V_{(8c)}$) in the main anionic motif to the number ($qF_{int(48i)}$) of interstitial fluorine anions $F_{int(48i)}$ in both crystals under study is approximately equal to 1.5, which is an additional argument in favor of the formation of the cuboctahedral anionic groups $\{F_{12}\}$ in $Ba_{0.69}La_{0.31}F_{2.31}$ crystals. The fraction of vacancies ($V_{(8c)}$) in 8*c* positions is calculated from the formula:

$$V_{(8c)} = 8 - qF_{(8c)} - qF_{int(32f)1}$$

where $qF_{(8c)}$ and $qF_{int(32f)1}$ are the numbers of matrix and relaxed anions in 8*c* and (32*f*)1, respectively.

Other interstitial anions in the ordered phases $Ba_4R_3F_{17}$ that correspond to $F_{int(4b)}$ anions in a disordered one occupy positions in the fluorine cubes outside $\{F_{12}\}$ groups. In the disordered phase, these anions may be located either outside clusters (inside fluorine cubes) or inside the cuboctahedron $\{F_{12}\}$.

The cationic motif in $Ba_4R_3F_{17}$ is distorted in the way that all R^{3+} cations are displaced from the center of the cluster along the four-fold axes, and Ba^{2+} cations are shifted towards the center of the cluster along three-fold axes. Based on displacements of cations in the octacubic clusters in $Ba_4R_3F_{17}$, similar displacements in the disordered phase $Ba_{0.69}La_{0.31}F_{2.31}$ should be assumed. The results of its structure refinement, however, showed the La^{3+} cations being shifted along the three-fold axis instead of Ba^{2+}. Therefore, we assume that inversed octacubic clusters are formed in both as-grown and annealed crystals in which La^{3+} cations are placed in the vertices of a cluster and Ba^{2+} in its faces (Figure 4). Such a cluster was also discovered in $Ba_{0.88}Yb_{0.22}F_{2.22}$ crystal [14]. Inversed arrangement of cations in the octacubic cluster is also found in $Ba_{0.75}Lu_{0.25}F_{2.25}$ [7] without formation of $\{F_{12}\}$ octahedron. The maximum number of R^{3+} cations in the octacubic cluster is six.

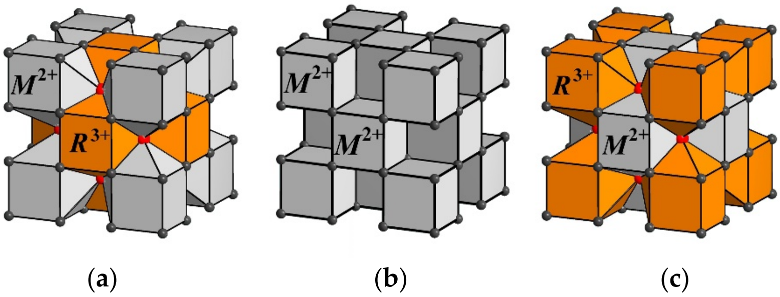

(**a**) (**b**) (**c**)

Figure 4. (**a**,**c**) Possible locations of cations in the octacubic $[M_{14-n}R_nF_{64+n}]$ cluster. (**b**) The fluorite structure.

According to the results of diffraction experiments, the octacubic cluster is formed in the phases $Ba_{1-x}R_xF_{2+x}$ with R = La–Nd, Ho–Lu and Y. The dependence of the cluster structure on the type of rare earth element and its concentration for the phases $Ba_{1-x}R_xF_{2+x}$ has not been systematically studied to date. The dependence of the defect structure on a thermal history of a crystal is crucial in the study of the structure of the $M_{1-x}R_xF_{2+x}$ fluorite phases. In situ studies of the evolution of the cluster structure of $Ca_{0.94}Y_{0.06}F_{2.06}$ up to 1200 °C are the most evident [15].

It is known that the time required to bring a fluorite crystal to an equilibrium state depends on the temperature of the heat treatment [16]. An in situ experiment does not provide comprehensive information on the dependence of the cluster structure on temperature, since such a study is carried out on crystals that are far from the equilibrium state. The results strongly depend on the duration of an experiment, and for comparison between them, the necessary condition is the unification of the thermal states of the initial crystals. We believe that the most effective method for studying the temperature dependence of the defect structure of the $M_{1-x}R_xF_{2+x}$ fluorite phases is fixing a thermal state of the crystals at different temperatures by annealing, and then conducting a diffraction experiment at low temperature to reduce thermal vibrations of ions.

This work is the first experimental study of the dependence of the defect structure on the thermal treatment of the $Ba_{1-x}R_xF_{2+x}$ phases. The task of the work included the elucidation of possible changes occurring in the cationic and anionic sublattices of $Ba_{0.69}La_{0.31}F_{2.31}$ during annealing. The authors needed to determine whether the type of the position occupied by interstitial anions and, accordingly, the type of cluster structure changes, and what modifications the atomic displacements of cations and anions undergo.

The changes occurring in the anionic sublattice of the heat-treated $Ba_{0.69}La_{0.31}F_{2.31}$ crystal consist of a ~1.7-fold decrease in the number of interstitial $F_{int(4b)}$ anions in the 4*b* site. During heat treatment, the number of $F_{int(48i)}$ anions did not change, but their atomic displacement parameter increased, which indicates the deformation of the anionic cuboctahedron $\{F_{12}\}$ as a result of annealing. In addition, thermal treatment led to the appearance of statically displaced matrix (relaxed) anions in the structure. No changes were found in the cationic sublattice as a result of annealing.

It should be noted that in the process of refining the structure of crystals with high symmetry, such as $M_{1-x}R_xF_{2+x}$ phases, strong correlations between refined parameters appear. They do not allow one to obtain occupancies of positions with high accuracy. Occupancies strongly correlate with the atomic displacement parameters, in particular for the positions of La^{3+} cations and relaxed $F_{int(32f)1}$ anions with small distances to neighboring ions. One of the tasks for further research is to conduct a diffraction experiment at low temperature to improve the accuracy of determining the occupancies of positions.

5. Conclusions

The structure of nonstoichiometric fluorite phase $Ba_{0.69}La_{0.31}F_{2.31}$ in as-grown condition and after a long isothermal annealing at 1173 K was studied by X-ray diffraction.

It was found that the crystals belong to the fluorite structure type.

In both crystals studied, vacancies in the matrix 8*c* anion position and interstitial fluorine ions at the 48*i* position ($F_{int(48i)}$) were found. The ratio of the number of the $F_{int(48i)}$ fluorine ions to the number of vacancies is approximately 1.5 in both crystals.

The displacements of the La^{3+} cations to the 32*f* site at (w, w, w) with $w \approx 0.023$ were found in both as-grown and annealed crystals.

It was established that annealing leads to a change in the type of displacement of the main anions in Wyckoff positions 8*c* from dynamic to static.

A model of the defect structure of $Ba_{0.69}La_{0.31}F_{2.31}$ is proposed, according to which interstitial fluorine anions and La^{3+} cations are aggregated into $[Ba_{14-n}La_nF_{64+n}]$ clusters with the cuboctahedral anionic core formed by interstitial fluorine anions in Wyckoff positions 48*i*. It is proposed that Ba^{2+} cations are located within the cluster in the centers of the faces, and the La^{3+} cations are shifted by 0.24 Å from the vertices of the cluster along the three-fold axis towards the center of the cluster.

Investigation of the structure-sensitive properties of $Ba_{0.69}La_{0.31}F_{2.31}$ crystals in connection with their defect cluster structure is in progress. The solution of this problem will provide the development of an approach to control the characteristics of these type of crystals.

Author Contributions: D.N.K. performed the annealing process and revised the manuscript. E.A.S. conducted diffraction experiments, refined the structures of the crystals and wrote the manuscript. B.P.S. grew the crystal, checked the analysis of the results and revised the manuscript. All authors have read and agreed to the published version of the manuscript.

Funding: This research was supported by the by the Ministry of Higher Education and Science of the Russian Federation within the State assignments of the Federal Scientific Research Centre «Crystallography and Photonics» of the Russian Academy of Sciences using the equipment of the Shared Research Center (project RFMEFI62119X0035).

Data Availability Statement: The data on the crystal structure of the $Ba_{0.69}La_{0.31}F_{2.31}$ samples investigated are deposited in the Cambridge Structural Database (CSD num. 2069418 for as-grown and 2069419 for annealed crystal).

Acknowledgments: Authors are grateful to Natalya A. Gubal for preparing the samples for X-ray diffraction experiments.

Conflicts of Interest: The authors declare no conflict of interest.

References

1. Sobolev, B.P. *The Rare Earth Trifluorides, Part 1: The High Temperature Chemistry of the Rare Earth Trifluorides*; Institut d'Estudis Catalans: Barcelona, Spain, 2000; 520p.
2. Bevan, D.J.M.; Greis, O.; Strahle, J. A New Structural Principle in Anion-Excess Fluorite-Related Superlattices. *Acta Cryst. A* **1980**, *36*, 889–890. [CrossRef]
3. Bevan, D.J.M.; Strahle, J.; Greis, O. The Crystal Structure of Tveitite, an Ordered Yttrofluorite Mineral. *J. Solid State Chem.* **1982**, *44*, 75–81. [CrossRef]
4. Golubev, A.M.; Otroshchenko, L.P.; Molchanov, V.N.; Sobolev, B.P. Displacements in the Cationic Motif of Nonstoichiometric Fluorite Phases $Ba_{1-x}R_xF_{2+x}$ as a Result of the Formation of $\{Ba_8[R_6F_{68-69}]\}$ Clusters: I. The $Ba_{0.78}Tm_{0.22}F_{2.22}$ Crystals. *Crystallogr. Rep.* **2008**, *53*, 966–973. [CrossRef]
5. Golubev, A.M.; Otroshchenko, L.P.; Molchanov, V.N.; Fykin, L.E.; Sobolev, B.P. Displacements in the Cationic Motif of Nonstoichiometric Fluorite Phases $Ba_{1-x}R_xF_{2+x}$ as a Result of the Formation of $\{Ba_8[R_6F_{68-69}]\}$ Clusters: II. The $Ba_{1-x}R_xF_{2+x}$ (R = Er, Yb, Lu; $0.1 < x < 0.3$) Crystals. *Crystallogr. Rep.* **2009**, *54*, 423–430. [CrossRef]
6. Otroshchenko, L.P.; Aleksandrov, V.B.; Muradian, L.A.; Sarin, V.A.; Sobolev, B.P. Neutron Diffraction Study of the Features of Fluorine Ions Incorporation into $Ba_{1-x}R_xF_{2+x}$ Solid Solutions. *Butll. Soc. Cat. Cien* **1991**, *12*, 383–391.

7. Sobolev, B.P.; Golubev, A.M.; Otroshchenko, L.P.; Molchanov, V.N.; Zakalyukin, R.M.; Ryzhova (Sulyanova), E.A.; Herrero, P. $Ba_{1-x}R_xF_{2+x}$ Phases (R = Gd − Lu) with Distorted Fluorite-type Structures—Products of Crystallization of Incongruent Melts in the $BaF_2 - RF_3$ Systems (R = Gd − Lu). III. Defect $Ba_{0.75}Lu_{0.25}F_{2.25}$ Structure. A New $\{Lu_8[Ba_6F_{71}]\}$ Supercluster of Defects. *Crystallogr. Rep.* **2003**, *48*, 944–952. [CrossRef]
8. Maksimov, B.A.; Solans, X.; Dudka, A.P.; Genkina, E.A.; Font-Badria, M.; Buchinskaya, I.I.; Loshmanov, A.A.; Golubev, A.M.; Simonov, V.I.; Font-Altaba, M.; et al. The Fluorite-Matrix-Based $Ba_4R_3F_{17}$ (R = Y, Yb) Crystal Structure. Ordering of Cations and Specific Features of the Anionic Motif. *Crystallogr. Rep.* **1996**, *41*, 50–57.
9. Sobolev, B.P.; Tkachenko, N.L. Phase diagrams of the BaF_2—$(Y,Ln)F_3$ systems. *J. Less-Common Metals* **1982**, *85*, 155–170. [CrossRef]
10. Karimov, D.N.; Buchinskaya, I.I.; Ivanova, A.G.; Il'ina, O.N.; Ivanovskaya, N.A.; Sorokin, N.I.; Sobolev, B.P.; Glushkova, T.M.; Ksenofontov, D.A. Growth of Fluorite Solid Solution Crystals in the Ternary SrF_2–BaF_2–LaF_3 System and Investigation of Their Properties. *Crystallogr. Rep.* **2018**, *63*, 1015–1021. [CrossRef]
11. Petricek, V.; Dusek, M.; Palatinus, L. Crystallographic Computing System JANA2006: General features. *Z. Kristallogr.* **2014**, *229*, 345–352. [CrossRef]
12. Becker, P.J.; Coppens, P. Extinction within the limit of validity of the Darwin transfer equations. I. General formalism for primary and secondary extinction and their applications to spherical crystals. *Acta Cryst. A* **1974**, *30*, 129–147. [CrossRef]
13. *International Tables for Crystallography*; Wilson, V.C.; Dordrecht, A.J.C. (Eds.) Kluwer: London, UK, 1992.
14. Maksimov, B.A.; Belokoneva, E.L.; Molchanov, V.N.; Grigor'eva, N.B.; Vigdorchik, A.G.; Krivandina, E.A.; Sobolev, B.P.; Gubina, Y.B. The $Ba_{1-x}R_xF_{2+x}$ (x = Gd − Lu) Phases with the Distorted Fluorite Structure as Products of Crystallization of Incongruent Melts in $BaF_2 - RF_3$ Systems. II. Crystal Structures of Two New Forms of $Ba_{1-x}Yb_xF_{2+x}$ Fluorite Phases and Some Features of the Anionic Packing and the Cation Distribution. *Crystallogr. Rep.* **2002**, *47*, 372–378. [CrossRef]
15. Hofmann, M.; Hull, S.; McIntyre, G.J.; Wilson, C.C. A neutron diffraction study of the superionic transition in $(Ca_{1-x}Y_x)F_{2+x}$ with x = 0.06. *J. Phys. Condens. Matter.* **1997**, *9*, 845–847. [CrossRef]
16. Fedorov, P.P. Anneal time determined by studying phase transitions in solid binary systems. *Russ. J. Inorg. Chem.* **1992**, *37*, 973–975.